

## Synthesis of new complex $[\text{Bi}_6\text{O}_6(\text{OH})_2](\text{ClC}_6\text{H}_4\text{SO}_3)_4$ and investigation of its thermal decomposition

Nikolay Kaloyanov<sup>a,\*</sup>, Alexander Zahariev<sup>b,\*</sup>, Veneta Parvanova<sup>c</sup>, Georgi Avdeev<sup>d</sup> & Christian Girginov<sup>e</sup>

<sup>a</sup>Department of Organic Chemistry, University of Chemical Technology and Metallurgy, 8 St. Kliment Ohridski blvd., 1756 Sofia, Bulgaria

<sup>b</sup>Department of Chemistry, Technical University, 8 St. Kliment Ohridski blvd., 1000 Sofia, Bulgaria,

<sup>c</sup>Department of General and Inorganic Chemistry, University of Chemical Technology and Metallurgy, 8 St. Kliment Ohridski blvd., 1756 Sofia, Bulgaria

<sup>d</sup>Institute of Physical Chemistry "Acad. Rostislav Kaischew", Bulgarian Academy of Sciences, Acad. G. Bonchev Str., bldg. 11, 1113, Sofia, Bulgaria

<sup>e</sup>Department of Physical Chemistry, University of Chemical Technology and Metallurgy, 8 St. Kliment Ohridski blvd., 1756 Sofia, Bulgaria

\*E-mail: nikolaykaloyanov@uctm.edu (Nikolay Kaloyanov), alexs\_zahariev@yahoo.com (Alexander Zahariev)

Received 1 April 2022; Accepted (revised) 20 February 2023

A new  $[\text{Bi}_6\text{O}_6(\text{OH})_2](\text{ClC}_6\text{H}_4\text{SO}_3)_4$  complex is synthesized through a reaction of  $\text{Bi}_2\text{O}_3$  with aqueous 4-chlorobenzenesulfonic acid at elevated temperature. The product composition is elucidated by elemental analysis, ICP-OES and FTIR techniques. By means of XRD analysis, the compound's indexation, monoclinic P2(3) space group and unit cell parameters:  $a=31.25(3)$  Å,  $b=19.78(1)$  Å,  $c=8.795(8)$  Å,  $\gamma = 94.33(4)^\circ$  as well as a cell volume =  $5424.21$  Å<sup>3</sup> are determined. Based on DTA-TG technique, three specific temperatures aimed at studying product's thermal decomposition are determined. The compositions of solid residues after isothermal heating are proved following the XRD and FTIR data.

**Keywords:** Bi(III) complexes, Thermal decomposition, TG-DTA, XRD, FTIR

Bismuth lies among few heavy metals, which are not only non-toxic to living organisms, but demonstrate numerous healing properties most of all in form of appropriate metal complexes. For example, Bi(III) oxido- and hydroxide oxido mono- and polycationic complexes with different anions of organic and inorganic acids have found an important medical application as modern antitumor and antimicrobial agents<sup>1-3</sup>. It is worth mention that bismuth complexes with different mono- and polycarboxylic acids are the first synthesized and most studied nowadays<sup>4-8</sup>. Recently, a few complexes containing anions of some sulfonic acids, e.g. sulfamic, sulfanillic, p-toluenesulfonic and 4-N-methylaminobenzene sulfonic ones have been reported as well<sup>9-12</sup>. Currently, some of the newest routes of synthesizing bismuth compounds comprising organic moieties appear to be the development of molecular oxido clusters having  $[\text{Bi}_{38}\text{O}_{45}]^{24+}$  core<sup>13</sup>.

In the last decade, various  $\text{Bi}^{3+}$  complexes mainly with  $\text{NO}_3^-$  ions appear to be functional as photocatalytic materials<sup>14</sup> and as encouraging materials for lithium-ion batteries<sup>15</sup>. Additionally, a contemporary subject of bismuth chemistry is the

synthesis of mixed oxide systems containing some other elements and related precursors with potential application in modern electronics<sup>16</sup>.

Despite the significant number of studies on the synthesis and properties of bismuth compounds comprising organic and inorganic anions, the interactions between Bi(III) and substituted benzenesulfonic acids remain insufficiently studied. In this respect, no information appears in the literature on the reaction between Bi(III) and 4-chlorobenzenesulfonic acid. Consequently, it will be of interest to carry out and study this reaction, as well as to characterize the product derived.

### Experimental Section

The interaction of  $\text{Bi}^{3+}$  (in a form of  $\text{Bi}_2\text{O}_3$ ) with 4-chlorobenzenesulfonic acid was performed in a following manner: 0.360 g  $\text{Bi}_2\text{O}_3$  (Merck  $\geq 99.5\%$ ) were added to 1.0 dm<sup>3</sup> 1% (pH 0.5) aqueous solution of  $\text{ClC}_6\text{H}_4\text{SO}_3\text{H}$  (TCI  $> 98\%$ ). The synthesis was carried out in a round-bottom flask equipped with a Graham condenser, during two weeks at a temperature of 95°C under vigorous stirring. The white precipitate obtained was washed out with

boiling double distilled water up to neutral reaction (pH 7.0) in order to remove any acid reminders and after that dried in a desiccator over  $P_4O_{10}$  under vacuum. The composition of new complex was elucidated by elemental analysis technique using EuroEA3000 Elemental Analyzer (Euro Vector SpA, Italy) performing in CHNS mode.

Fourier-transform infrared (FTIR) spectra were recorded by Varian 660-IR FTIR Spectrometer within the range  $4000-450\text{ cm}^{-1}$ . The samples were analyzed in the form of KBr pellets. ICP-OES analysis was realized using "Prodigy" ICP-OES high dispersion Spectrometer (Tellelyne Leeman Labs, USA). Powder XRD patterns were plotted by employing PANalytical Empyrean provided with a Pixel 3D multichannel detector ( $CuK\alpha$  45 kV – 40 mA radiation) within  $3-90^\circ$   $2\theta$  range and scan step  $0.026^\circ/33$  seconds. Diverse search-match software along with Inorganic Crystal Structure Database (ICSD) were applied for phase identification.

LABSYS<sup>TM</sup>evo(SETARAM) was in operation to carry out DTA-TG measurements within  $20-920^\circ\text{C}$  temperature range at a heating rate  $10^\circ\text{C min}^{-1}$  in Ar atmosphere ( $20\text{ cm}^3\text{ min}^{-1}$  flow rate). Both an empty alumina crucible (reference) and sample mass  $23.0\text{ mg}$  ( $\pm 0.01\%$  weighing precision) were used.

Isothermal investigations at three characteristic temperatures ( $369^\circ\text{C}$ ,  $558^\circ\text{C}$  and  $662^\circ\text{C}$ ) derived from DTA and TG analysis were performed in air atmosphere. All samples ( $m = 40.0\text{ mg}$ ) were heated for 60 min at these temperatures, which were maintained within  $\pm 1^\circ\text{C}$ . After heating, the samples were cooled out to room temperature in a desiccator over  $P_4O_{10}$ . The composition of each of three solid residuals derived after isothermal heating was identified by elemental analysis, FTIR and powder XRD techniques.

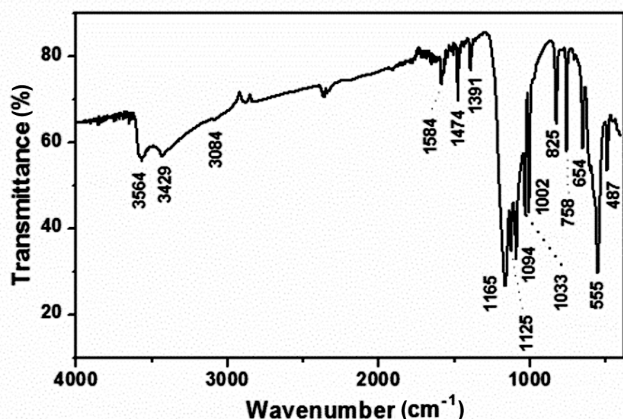


Fig. 1 — FTIR spectrum of  $[Bi_6O_6(OH)_2](ClC_6H_4SO_3)_4$

## Results and Discussion

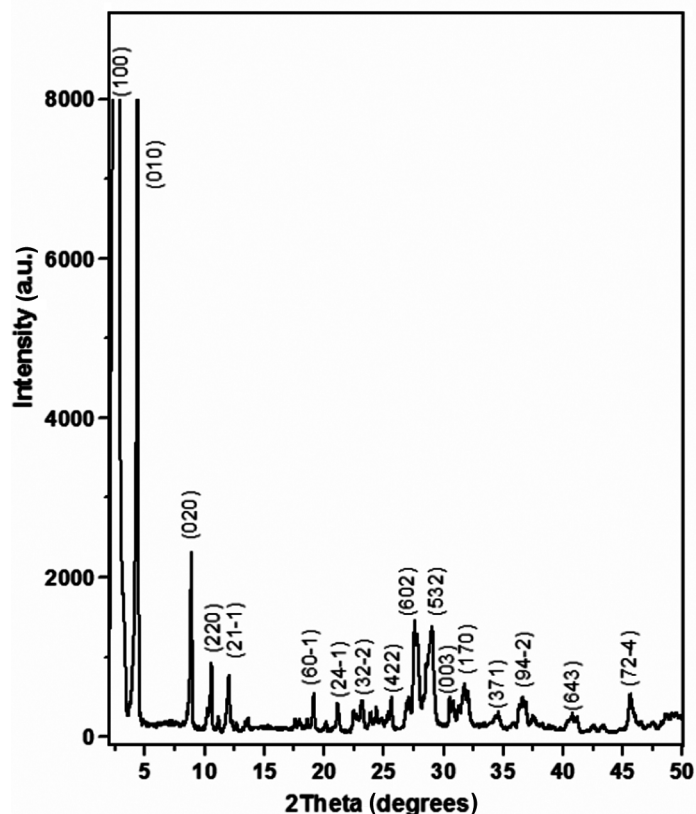
The elemental analysis of new compound synthesized is presented as Calcd. %: C – 13.39; H – 0.83 and Found %: C – 13.53; H – 0.78. The experimental values found are within  $\pm 0.40\%$  of the theoretical ones. The bismuth content is evaluated by means of ICP-OES technique and appears as %Bi = 58.33 (Calcd) and 58.73 (Found).

FTIR spectrum of the product synthesized is presented in Fig. 1 and the assignments are given in Table 1. It is visible that stretching vibrations of two different –OH groups appear at  $3564$  and  $3429\text{ cm}^{-1}$ . The signals coming from p-disubstituted aromatic ring are also present as follows:  $3084\text{ cm}^{-1}$  for  $\nu\text{C-H}$ ,  $1584$  and  $1474\text{ cm}^{-1}$  for  $\nu\text{C=C}$  and  $825\text{ cm}^{-1}$  for out of plane  $\gamma\text{C-H}$  bond. Furthermore, there are bands at  $1391$  and  $1165\text{ cm}^{-1}$ , responsible for  $\nu_{as}\text{SO}_2$  followed by a band that appears at  $1033\text{ cm}^{-1}$  corresponding to  $\nu_s\text{SO}_2$  as well. Another important signals originated from stretching and bending vibrations of  $\text{C(Ar)-Cl}$  bond are situated at  $758$  and  $654\text{ cm}^{-1}$ , respectively. On the other hand, bands characteristic for the cationic structure are distinguishable at  $1125$  and  $1094\text{ cm}^{-1}$ , due to  $\delta\text{Bi-OH}$  as well as at  $555$  and  $487\text{ cm}^{-1}$  for  $\nu\text{Bi-O}$  and  $\delta\text{Bi-O}$ , respectively.

The XRD pattern of this compound is presented in Fig. 2. From this figure, it could be ascertained that any known Bi(III)-containing phases are identified. This allows to perform indexation of XRD data, which represents monoclinic P2(3) space group with unit cell parameters:  $a=31.25(3)\text{ \AA}$ ,  $b=19.78(1)\text{ \AA}$ ,  $c=8.795(8)\text{ \AA}$ ,  $\gamma=94.33(4)^\circ$  and a cell volume  $=5424.21\text{ \AA}^3$ . The experimental and calculated values of various diffraction parameters are summarized in Table 2.

Table 1 — FTIR spectral data and band assignments of  $[Bi_6O_6(OH)_2](ClC_6H_4SO_3)_4$

Wavenumber ( $\text{cm}^{-1}$ )	Assignment
3564	$\nu\text{OH}$
3429	$\nu\text{OH}$
3084	$\nu\text{C-H (Ar)}$
1584,1474	$\nu\text{C=C(Ar)}$
1391	$\nu_{as}\text{SO}_2$
1165	$\nu_{as}\text{SO}_2$
1125	$\delta\text{Bi-OH}$
1094	$\delta\text{Bi-OH}$
1033	$\nu_s\text{SO}_2$
1002	$\nu\text{S=O}$
825	$\gamma\text{C-H p-disubstitutedAr}$
758	$\nu\text{C(Ar)-Cl}$
654	$\delta\text{C(Ar)-Cl}$
555	$\nu\text{Bi-O}$
487	$\delta\text{Bi-O}$

Fig. 2 — XRD pattern of  $[\text{Bi}_6\text{O}_6(\text{OH})_2](\text{ClC}_6\text{H}_4\text{SO}_3)_4$ Table 2 — X-ray diffraction data from indexing  $[\text{Bi}_6\text{O}_6(\text{OH})_2](\text{ClC}_6\text{H}_4\text{SO}_3)_4$ 

h k l	$2\theta(\text{c}) [^\circ]$	$2\theta(\text{o}) [^\circ]$	$2\theta(\text{d}) [^\circ]$	d-sp. (c) [ $\text{\AA}$ ]	d-sp. (o) [ $\text{\AA}$ ]	d-sp. (d) [ $\text{\AA}$ ]
1 0 0	2.8316	2.8594	-0.0277	31.17586	30.87369	0.302169
0 1 0	4.4629	4.4429	0.0199	19.78369	19.87247	-0.08879
0 2 0	8.9325	8.9236	0.0089	9.891844	9.901709	-0.00987
1 0 -1	10.2598	10.2549	0.0048	8.615002	8.619031	-0.00403
2 2 0	10.5836	10.587	-0.0034	8.352095	8.349428	0.002667
2 1 -1	12.0487	12.0317	0.017	7.339628	7.349957	-0.01033
3 0 -1	12.6952	12.6933	0.0018	6.967269	6.968278	-0.00101
6 1 0	17.6338	17.6411	-0.0073	5.025538	5.023464	0.002074
6 0 -1	19.1693	19.1614	0.0079	4.626289	4.628181	-0.00189
1 0 -2	20.2164	20.1957	0.0207	4.388968	4.393421	-0.00445
2 4 -1	21.1736	21.1706	0.003	4.192672	4.193258	-0.00059
2 2 -2	22.4949	22.4933	0.0016	3.949302	3.949577	-0.00028
3 2 -2	23.2024	23.2148	-0.0124	3.830464	3.828443	0.002021
6 4 0	24.8335	24.8173	0.0162	3.582434	3.584738	-0.0023
4 2 2	25.6576	25.6392	0.0184	3.469213	3.471656	-0.00244
6 0 2	27.5652	27.5648	0.0004	3.233311	3.233355	-4.4E-05
5 3 2	29.0805	29.0769	0.0035	3.068191	3.068554	-0.00036
0 0 3	30.5502	30.5181	0.032	2.923852	2.926847	-0.003
1 7 0	31.7656	31.768	-0.0025	2.814699	2.814485	0.000214
3 7 1	34.6086	34.6394	-0.0309	2.589708	2.587471	0.002237
9 4 -2	36.6125	36.6109	0.0016	2.452431	2.452537	-0.00011
6 4 3	40.8065	40.8144	-0.0079	2.209532	2.209123	0.000409
7 2 -4	45.6043	45.6208	-0.0165	1.98761	1.986928	0.000681

In view of the data derived from elemental analysis, ICP-OES, FTIR spectrum and XRD pattern, the composition of new complex synthesized can be written as  $[\text{Bi}_6\text{O}_6(\text{OH})_2](\text{ClC}_6\text{H}_4\text{SO}_3)_4$ . From XRD technique is obvious that none of certain phases are detected, which along with the data mentioned above, points at high purity of the substance.

In Fig. 3, DTA and TG curves of thermal analysis of  $[\text{Bi}_6\text{O}_6(\text{OH})_2](\text{ClC}_6\text{H}_4\text{SO}_3)_4$  are presented. In DTA curve a weak endothermic effect at  $T_{\text{max}} = 251^\circ\text{C}$  and a weaker exothermic one at  $T_{\text{max}} = 350^\circ\text{C}$  are registered within the range  $T = 20\text{--}369^\circ\text{C}$ . Based on the thermogravimetric data, a mass loss,  $\Delta m = 2.5\%$ , within the same temperature range is found out. This process is related to started decomposition of complex synthesized resulting information of both amorphous and new crystalline phase, which is visible in XRD pattern of isothermally heated sample of the complex at  $T = 369^\circ\text{C}$  (Fig. 4a). The crystalline phase inherits some diffraction lines of the initial compound, whereby the short-range order of structural elements is retained, whereas the long-range one is lost. This observation is also confirmed by the weak exothermic effect, corresponding to structural changes occurred. In FTIR spectrum of the same sample (Fig. 5a), absorption bands of the same functional groups as in starting compound are observed due to the retention of short-range order of structural elements.

The second stage of thermal decomposition takes place in the range  $T = 369\text{--}558^\circ\text{C}$  (Fig. 3). An endothermic effect is observed in the DTA curve, with

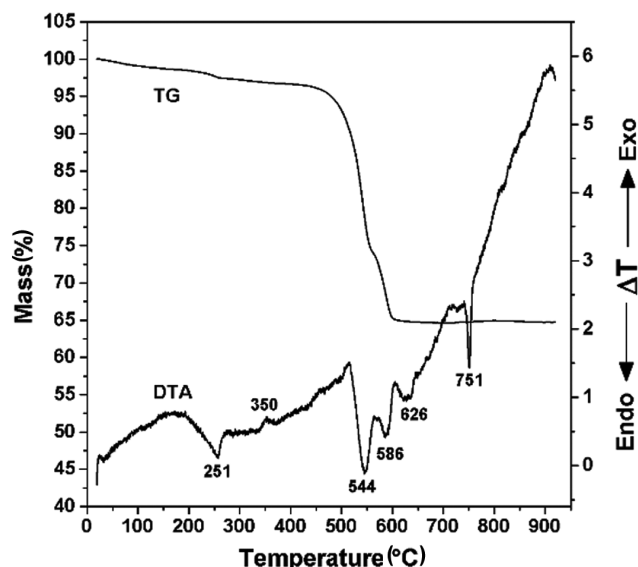


Fig. 3 — DTA-TG curves of  $[\text{Bi}_6\text{O}_6(\text{OH})_2](\text{ClC}_6\text{H}_4\text{SO}_3)_4$

$T_{\text{max}} = 544^\circ\text{C}$ . From the TG curve, a decrease in mass  $\Delta m = 22.2\%$  is calculated. The main mass loss corresponding to the significantly greater endothermic effect occurs in the temperature range considered. These processes are related to decomposition of aromatic ring from the anion,  $(\text{ClC}_6\text{H}_4\text{SO}_3)^-$ , of  $-\text{OH}$  groups from the cation,  $[\text{Bi}_6\text{O}_6(\text{OH})_2]^{4+}$  and of the amorphous phase. This conclusion is confirmed by FTIR spectrum of an isothermally heated sample at  $T = 558^\circ\text{C}$  (Fig. 5b). In this figure absorption bands for  $\nu\text{C-H}$  at  $3084\text{ cm}^{-1}$ , for  $\nu\text{C}=\text{C}(\text{Ar})$  at  $1585$  and  $1479\text{ cm}^{-1}$ , for out of plane  $\gamma\text{C-H}$  from *p*-disubstituted aromatic ring at  $825\text{ cm}^{-1}$ , for  $\nu\text{C}(\text{Ar})-\text{Cl}$  at  $758$  and  $\delta\text{C}(\text{Ar})-\text{Cl}$  at  $654\text{ cm}^{-1}$ , for  $\nu\text{O-H}$  at  $3534\text{ cm}^{-1}$  as well as for  $\delta\text{Bi-OH}$  at  $1129\text{ cm}^{-1}$  are not

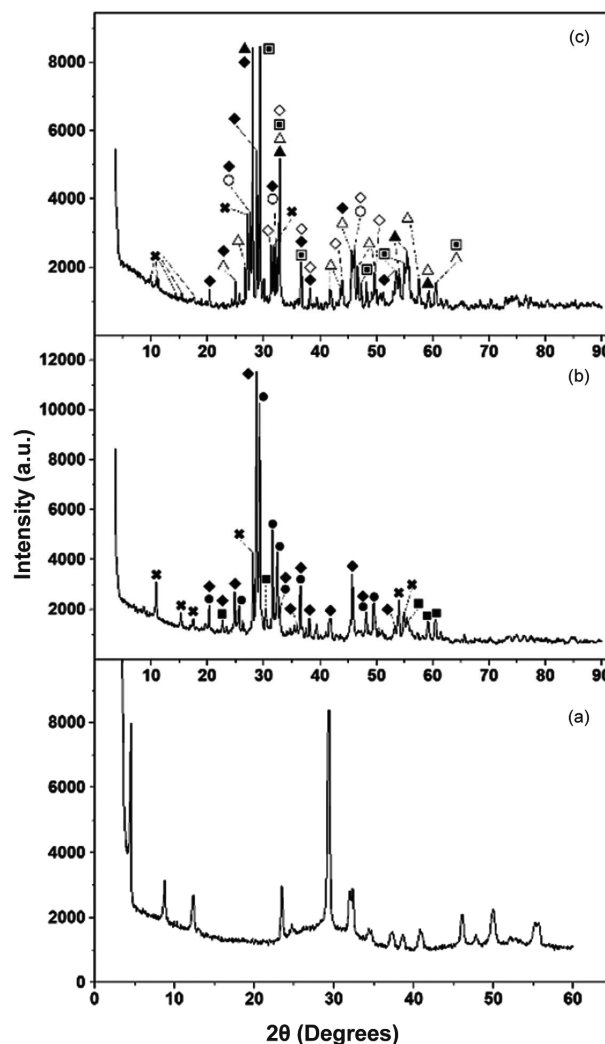


Fig. 4 — XRD patterns for solid residuals after isothermal heating at three temperatures: a)  $369^\circ\text{C}$ ; b)  $558^\circ\text{C}$ ; c)  $662^\circ\text{C}$ . The phases are denoted as follows:  $\blacksquare$  -  $\text{Bi}_2\text{O}_3$ ,  $\bullet$  -  $\text{Bi}_{34.7}\text{O}_{36}(\text{SO}_4)_{16}$ ,  $\blacklozenge$  -  $\text{Bi}_{28}\text{O}_{72}\text{S}_{10}$ ,  $\triangle$  -  $\alpha\text{-Bi}_2\text{O}_3$ ,  $\blacktriangle$  -  $\beta\text{-Bi}_2\text{O}_3$ ,  $\square$  -  $\text{Bi}_2\text{O}_{2.3}$ ,  $\circ$  -  $\text{Bi}_2\text{O}_3$ -defective,  $\diamond$  -  $\text{Bi}_8\text{O}_{15}\text{S}$  and  $\times$  - unknown crystalline phase

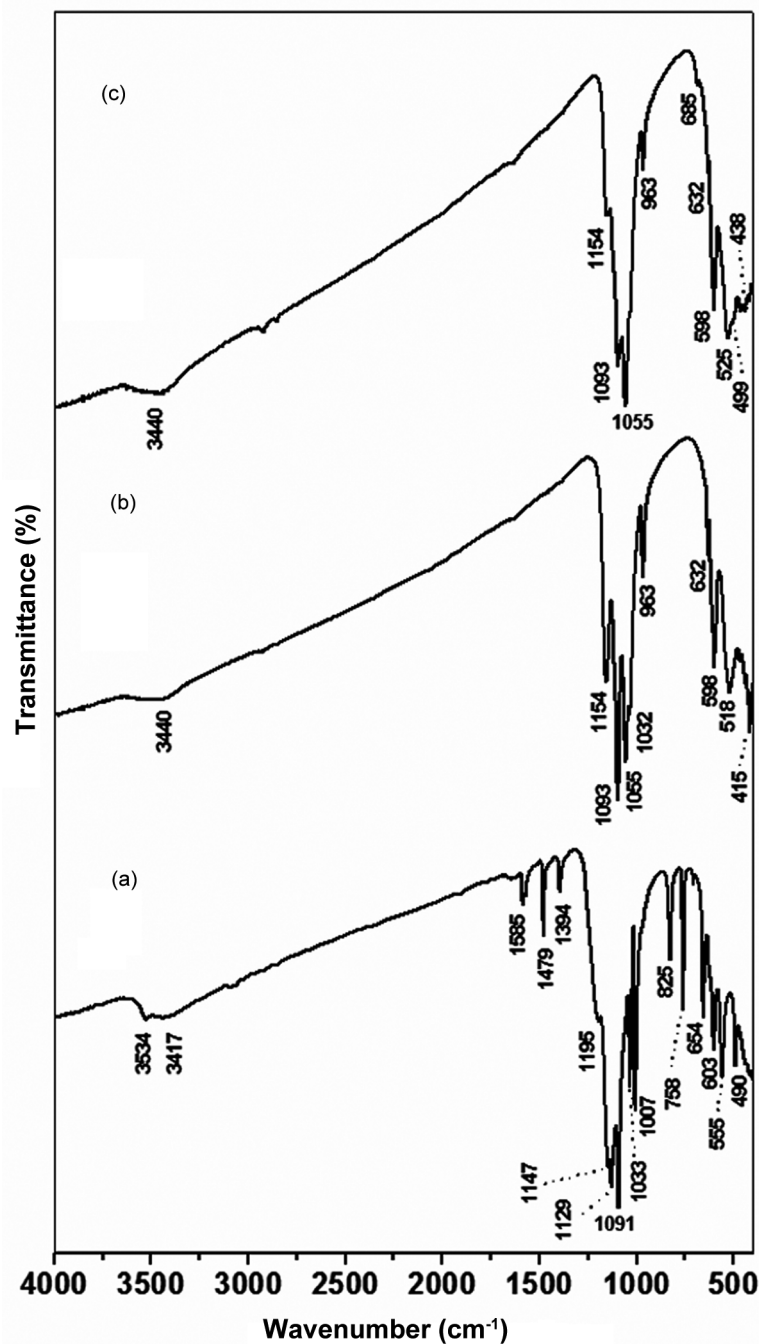


Fig. 5 — FTIR spectra of solid residues after isothermal heating at three temperatures: (a) 369°C, (b) 558°C and (c) 662°C

visible. XRD analysis of the same sample shows formation of  $\text{Bi}_2\text{O}_3$  (ICDD: 98-002-7151),  $\text{Bi}_{34.7}\text{O}_{36}(\text{SO}_4)_{16}$  (ICDD:98-004-9900),  $\text{Bi}_{28}\text{O}_{72}\text{S}_{10}$  (ICDD:98-004-9901) and an unknown crystalline phase. The absence of an exothermic effect corresponding to structural transformations can be explained by overlap of both types of effects, with the predominant role of larger endothermic one.

The third stage of TG curve covers temperature range from 558 to 662°C. The decrease in sample weight at this stage is  $\Delta m = 7.2\%$ . In DTA curve two endothermic effects with  $T_{\text{max}} = 586^\circ\text{C}$  and  $T_{\text{max}} = 626^\circ\text{C}$  correspond to this stage (Fig. 3). These processes are related to the complete decomposition of  $\text{Bi}_{34.7}\text{O}_{36}(\text{SO}_4)_{16}$ . In XRD pattern of isothermally heated sample at  $T = 662^\circ\text{C}$ , diffraction lines of  $\alpha\text{-Bi}_2\text{O}_3$  (ICDD: 98-016-8806),

$\beta$ - $\text{Bi}_2\text{O}_3$  (ICDD: 98-041-7638),  $\text{Bi}_2\text{O}_{2.3}$  (ICDD:98-003-7366),  $\text{Bi}_2\text{O}_3$ -defective (ICDD:98-016-8809),  $\text{Bi}_{28}\text{O}_{72}\text{S}_{10}$  (ICDD:98-004-9901),  $\text{Bi}_8\text{O}_{15}\text{S}$  (ICDD:98-005-5744) and an unknown crystalline phase are registered (Fig. 4c). FTIR spectrum of the same sample confirms the presence of functional groups contained in the phases formed at  $T = 662^\circ\text{C}$ . The absorption bands of  $\nu_{\text{as}}\text{SO}_2$  at  $1154\text{ cm}^{-1}$ ,  $\nu_{\text{s}}\text{SO}_2$  at  $1055\text{ cm}^{-1}$  as well as of  $\nu\text{Bi-O}$  and  $\delta\text{Bi-O}$  at  $525$  and  $499\text{ cm}^{-1}$ , respectively, are clearly observable. At this third stage of decomposition, structural transformations are not expressed by exothermic effects as well, for the same reasons as in previous stage.

In temperature range  $T = 662 - 900^\circ\text{C}$ , in DTA curve a sharp endothermic effect is registered with  $T_{\text{max}} = 751^\circ\text{C}$  (Fig. 3). In TG curve no mass loss corresponds to this effect, which can be explained by a melting process.

An elemental analysis of carbon and hydrogen content is performed on the three isothermally heated samples. At  $T = 369^\circ\text{C}$ ,  $C = 9.99\%$  and  $H = 0.77\%$ , which are present in unknown crystalline and amorphous phases formed. At  $T = 558^\circ\text{C}$ ,  $C = 1.36\%$  and  $H = 0.36\%$ , while at  $T = 662^\circ\text{C}$ ,  $C = 0.40\%$  and  $H = 0.21\%$ , which results can be explained by presence of unknown crystalline phases as well as by increasing temperature.

### Conclusion

A new complex having the composition  $[\text{Bi}_6\text{O}_6(\text{OH})_2](\text{ClC}_6\text{H}_4\text{SO}_3)_4$  is derived using  $\text{Bi}_2\text{O}_3$  and  $\text{ClC}_6\text{H}_4\text{SO}_3\text{H}$  as starting compounds, accompanied by optimization of the synthesis conditions. The composition of the compound is revealed through elemental analysis, FTIR and ICP-OES methods. X-ray

powder diffraction points out that the complex is well crystallized and comprises any known phases, hence an indexation and unit cell parameters determination is carried out. Based on DTA-TG analysis, three characteristic temperatures are outlined and the composition of solid residues resulting from isothermal heating at these temperatures is revealed by XRD, FTIR and elemental analysis.

### References

- 1 Yang N & Sun H, *Coord Chem Rev*, 251 (2007) 2354.
- 2 Stavila V, Davidovich R L, Gulea A & Whitmire K H, *Coord Chem Rev*, 250 (2006) 2782.
- 3 Briand G G & Burford N, *Chem Rev*, 99 (1999) 2601.
- 4 Kulakov V N, Klimova T P, Gol'tyapin Yu V, Babushkina T A, Klemenkova Z S, Lipengol'ts A A & Nekrasov M S, *Russ J Coord Chem*, 36 (2010) 333.
- 5 Chen X, Cao Y, Zhang H, Chen Y, Chen X & Chai X, *J Solid State Chem*, 181 (2008) 1133.
- 6 Anjaneyulu O & Swamy K C K, *J Chem Sci*, 123 (2011) 131.
- 7 Andrews P C, Deacon G B, Junk P C, Kumara I & Silberstein M, *Dalton Trans*, (2006) 4852.
- 8 Bokhonov B B & Yukhin Yu M, *Russ J Inorg Chem*, 55 (2010) 1381.
- 9 Zahariev A, Parvanova V & Kaloyanov N, *Thermochim Acta*, 502 (2010) 90.
- 10 Zahariev A, Kaloyanov N, Girginov C & Parvanova V, *Thermochim Acta*, 528 (2012) 85.
- 11 Zahariev A, Kaloyanov N, Parvanova V & Girginov C, *Thermochim Acta*, 594 (2014) 11.
- 12 Zahariev A, Kaloyanov N, Parvanova V & Girginov C, *Thermochim Acta*, 683 (2020) 178436.
- 13 Weber M, Thiele G, Dornsiepen E, Weimann D P, Schalley C A, Dehnen S & Mehring M, *Z Anorg Allg Chem*, 644 (2018) 1796.
- 14 Yang Y, Liang H, Zhu N, Zhao Y, Guo C & Liu L, *Chemosphere*, 93 (2013) 701.
- 15 Wu K, Shao L, Jiang X, Shui M, Ma R, Lao M, Lin X, Wang D, Long N, Ren Y & Shu J, *J Power Sources*, 254 (2014) 88.
- 16 Matskevich N I, Wolf T, Adelman P, Fuchs D, Semerikova A & Matskevich M Y, *J Chem Thermodyn*, 116 (2018) 147.